

Determination of Intermolecular Hydrogen Bonded Conformers of α -Aryloxypropanoic Acids Using Density Functional Theory Predictions of Vibrational Absorption and Vibrational Circular Dichroism Spectra

Jiangtao He and Prasad L. Polavarapu*

Department of Chemistry, Vanderbilt University, Nashville, Tennessee 37235

Received October 29, 2004

Abstract: The density functional theoretical predictions of vibrational absorption (VA) and vibrational circular dichroism (VCD) spectra for monomeric chiral α -aryloxypropanoic acids are found to be in serious disagreement with corresponding experimental spectra. This disagreement made it difficult to establish the predominant conformations and absolute configuration of chiral α -aryloxypropanoic acids. Since carboxylic acids tend to form dimers through intermolecular hydrogen bonding in solution, such hydrogen bonding should be either eliminated in the experimental measurements or modeled properly in the theoretical calculations for achieving agreement between theoretical predictions and experimental observations. Esterification eliminates hydrogen bonding in solution, but this approach does not provide information about the conformations of the acids. As a consequence, the option to properly model the dimers of α -aryloxypropanoic acids and to evaluate the dimer conformations in reproducing the experimental spectra becomes important. Here we report a method for obtaining the dimer conformations of α -aryloxypropanoic acids using density functional theory and evaluate their reliability by comparing the predicted and experimental VA and VCD spectra. The population weighted predicted VA and VCD spectra of dimers matched well with the corresponding experimental spectra in solution, thereby indicating the predominant dimer conformers and absolute configuration of α -aryloxypropanoic acids.

Introduction

α -Aryloxypropanoic acids are an important class of chiral chemicals used as herbicides. These herbicides include 2-(4-chloro-2-methylphenoxy)propanoic acid and 2-(2,4-dichlorophenoxy)propanoic acid, which are marketed under brand names Mecoprop and Dichloroprop, respectively. Each of these two compounds can exist in two enantiomeric forms. Only their (+)-enantiomers are herbicidally active, while the (–)-enantiomers are devoid of herbicidal activity but are powerful antiauxins.^{1–3} These compounds may undergo racemization by inversion of the absolute configuration at the asymmetrically substituted C-atom.⁴ It was also found that microbial degradation of racemic herbicides preferentially eliminates one enantiomer over the other.⁵ To understand such biological interactions at the molecular level it is

necessary to know the absolute configuration and predominant conformations of chiral herbicides.

Two other α -aryloxypropanoic acids of importance are 2-(2-chlorophenoxy)propanoic acid and 2-(3-chlorophenoxy)propanoic acid, which are closely related to Mecoprop and Dichloroprop. To eliminate the influence of hydrogen bonding effects in solution, methyl esters of propanoic acids, namely methyl 2-(4-chloro-2-methylphenoxy)propanoate, methyl 2-(2,4-dichlorophenoxy)propanoate, methyl 2-(2-chlorophenoxy)propanoate, and methyl 2-(3-chlorophenoxy)propanoate, have been synthesized^{6,7} and subjected to experimental and theoretical investigations. From these investigations the absolute configurations of esters, and those of parent acids there from, have been determined. Although these prior studies helped in determining the absolute configurations and provided insight into the conformations of esters, they did not provide any information on the

* Corresponding author phone: (615)322-2836; fax: (615)322-4936; e-mail: Prasad.L.Polavarapu@vanderbilt.edu.

predominant conformations of parent acids. The objective of this manuscript is to determine the predominant conformations of α -aryloxypropanoic acids.

Hydrogen bonding plays a very important role in the structures of molecules ranging from water⁸ to biological molecules such as DNA⁹ and proteins.¹⁰ This is also the case for small carboxylic acids such as formic acid, acetic acid, and propanoic acid. The experimental and theoretical studies show that these carboxylic acids tend to form dimers through intermolecular hydrogen bonding.¹¹ There are also several efforts in understanding hydrogen bonding using different theoretical methods, including ab initio and density functional theory (DFT).¹²

Vibrational circular dichroism (VCD) is an important chiroptical technique for studying the absolute configuration and conformations of chiral molecules.^{13–16} The combination of experimental VCD spectra and corresponding density functional theory predictions provides a powerful method for determining the absolute configuration and predominant conformations of chiral molecules.¹⁶ But, most theoretical VCD spectral calculations to date have dealt with monomer molecules. The calculations for dimer molecules with flexible structure are less common because such studies will require much more computational effort. A few attempts have been made to investigate dimers, where monomers have only a limited number of possible starting conformation.¹⁷ For monomers with several possible starting conformations, we are not aware of any attempts trying to address intermolecular hydrogen bonded dimers. In the present study, we address this problem and suggest an approach to deal with monomers possessing several possible starting conformations.

In this manuscript we report investigations for four α -aryloxypropanoic acids, which are 2-(2-chlorophenoxy)propanoic acid **1**, 2-(3-chlorophenoxy)propanoic acid **2**, 2-(4-chloro-2-methylphenoxy)propanoic acid **3**, and 2-(2,4-dichlorophenoxy)propanoic acid **4**. We have optimized the dimer conformations of these propanoic acids and calculated their VA and VCD spectra. The good agreement obtained between the population weighted predicted spectra for dimer conformations and the experimental spectra in solution further validates the predominant conformations of four acids investigated.

Although the biological or agricultural relevance of compounds **1–4** relates to their use in aqueous environments, infrared absorption or VCD spectroscopy is not a convenient technique for studying aqueous solutions due to strong absorption of infrared radiation by water. Furthermore, in aqueous environments intermolecular hydrogen bonding between solute and solvent molecules becomes as important as intermolecular hydrogen bonding between solute molecules. These competing hydrogen-bonding effects make it difficult to obtain reliable theoretical predictions. For this reason, the present experimental investigations are carried out in CDCl_3 solvent, which is not expected to interfere with intermolecular hydrogen bonding between solute molecules. As a result, it is sufficient to carry out the theoretical predictions in a vacuum without explicit inclusion of solvent influence.

Experimental Methods

Racemic **1** and **2** were obtained from TCI America and Aldrich Chemical Co., respectively. The enantiomers of **1** and **2** were separated⁷ in-house at 25 °C on a 4.6×250 mm chiral column (Chiralpak AD-H column from Daicel Chemical Industries, Ltd.) using a mobile phase of 3% 2-propanol in hexane, with 0.03% trifluoroacetic acid, run at 1 mL/min with UV detection at 254 nm. The experimental specific rotations of the first elutants of **1** and **2**, respectively, are $[\alpha]_D^{20} = -26.6$ ($c=1.23$, CH_3COCH_3) and $[\alpha]_D^{20} = -49.7$ ($c=0.58$, CH_3COCH_3). The experimental specific rotations of the second elutants of **1** and **2**, respectively, are $[\alpha]_D^{20} = +28.5$ ($c=0.97$, CH_3COCH_3) and $[\alpha]_D^{20} = +53.5$ ($c=0.79$, CH_3COCH_3). Analytical grade samples of (+)-enantiomers of **3** ($[\alpha]_D^{20} = +16.3$ ($c=2.31$, CHCl_3)) and **4** ($[\alpha]_D^{20} = +19.0$ ($c=2.29$, CHCl_3)) were obtained⁶ as a gift from A. H. Marks Co. (U.K.).

The infrared and VCD spectra were recorded on a commercial Fourier transform VCD spectrometer, Chiralir (Bomem-BioTools, Canada). A second PEM was added to improve the signal/noise ratio and reduce the artifacts.¹⁸ The VCD spectra were recorded with 3-h data collection time at 4 cm^{-1} resolution. Spectra were measured in CDCl_3 solvent. The concentrations are 0.150 M for **1** (path length 180 μm); 0.150 M for **2** (path length 180 μm); 0.158 M for **3** (path length 120 μm); and 0.155 M for **4** (path length 70 μm). The sample was held in a variable path length cell with BaF_2 windows. In both the absorption and VCD spectra presented, the corresponding solvent spectra obtained under identical conditions were subtracted out.

Theoretical Calculations

The geometry optimization, vibrational frequencies, absorption intensities, and VCD intensities were calculated by Gaussian 03 program.¹⁹ The calculations used the density functional theory with B3LYP functional and 6-31G* basis set. The procedure for calculating the VCD intensities using DFT theory is as implemented in Gaussian 03 program.¹⁹ The theoretical absorption and VCD spectra were simulated with Lorentzian band shapes and 5 cm^{-1} bandwidths. Because the predicted band positions are higher than the experimental band positions, the calculated B3LYP/6-31G* frequencies were scaled with 0.9613, as recommended by Wong.²⁰ The use of larger basis sets can overcome the need for arbitrary scaling of frequencies, but such larger basis sets also would require more computational resources than are available to us. One approach to lower the time demands involved in geometry optimization calculations is to do the conformational search using Monte Carlo methods using empirical force fields. However, for consistency all calculations here were carried out at B3LYP/6-31G* level of theory.

Results and Discussion

The results will be divided into two sections, one on monomer conformations and the other on dimer conformations. The results on monomeric acid conformations have been reported^{6,7} before, but first we briefly summarize those results for clarity and completeness.

Monomer Conformations. The conformational flexibility in these acids arises from the rotation around four single

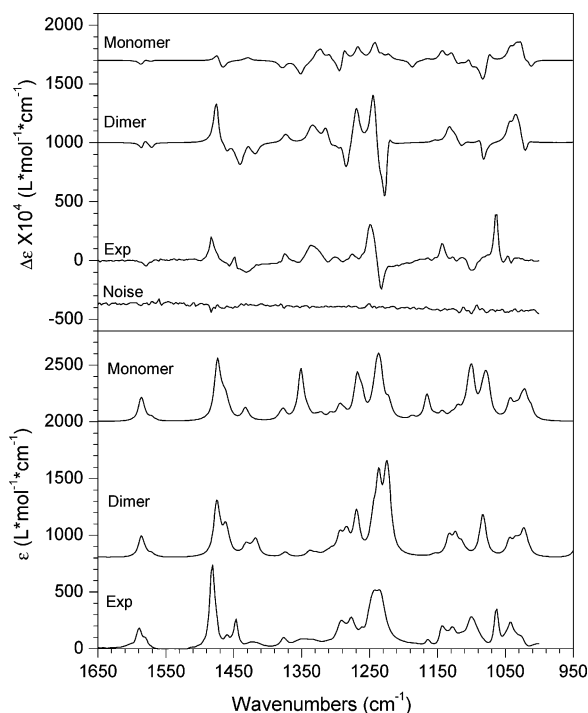
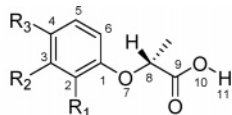


Figure 1. Comparison between experimental and B3LYP/6-31G* predicted vibrational absorption (bottom panel) and VCD (top panel) spectra of 2-(2-chlorophenoxy)propanoic acid. The predicted frequencies are scaled by 0.9613. The experimental measurements were made for (+)-enantiomer and calculations were done for (*R*)-configuration. The trace labeled “noise” represents the reproducibility level in the experimental VCD spectrum.

Chart 1. Structure and Atomic Numbering of α -Aryloxypropanoic Acids



1, $R_1=Cl$, $R_2=H$, $R_3=H$; 2, $R_1=H$, $R_2=Cl$, $R_3=H$;

3, $R_1=CH_3$, $R_2=H$, $R_3=Cl$; 4, $R_1=Cl$, $R_2=H$, $R_3=Cl$;

bonds: C^1O^7 , O^7C^8 , C^8C^9 , and C^9O^{10} (see Chart 1). The initial dihedral angles D1, D2, D3, and D4, respectively, representing the segments (see Chart 1) $C^2C^1O^7C^8$, $C^1O^7C^8C^9$, $O^7C^8C^9O^{10}$, and $C^8C^9O^{10}H^{11}$ are varied in 120° increments. This resulted in $3^4 = 81$ possible conformations for each of the four acids. All these conformations have been subjected to geometry optimizations. (A) (*R*)-2-(2-Chlorophenoxy)propanoic acid, (*R*)-1: For this acid, four lowest energy stable conformers, labeled Con1, Con2, Con3, and Con4, with fractional populations of 0.28, 0.27, 0.24, and 0.21 are found. The four dihedral angles, D1, D2, D3, and D4, for these conformers are as follows: 177, 71, 35, and 178 for Con1; -164, 146, -4, and 1 for Con2; 177, 73, -159, and -176 for Con3; 81, 80, -169, and -178 for Con4. The population weighted predicted vibrational absorption and VCD spectra are compared to the experimental spectra in Figure 1. From this figure it is evident that the predicted spectra of monomeric (*R*)-1 do not compare well⁷ with the

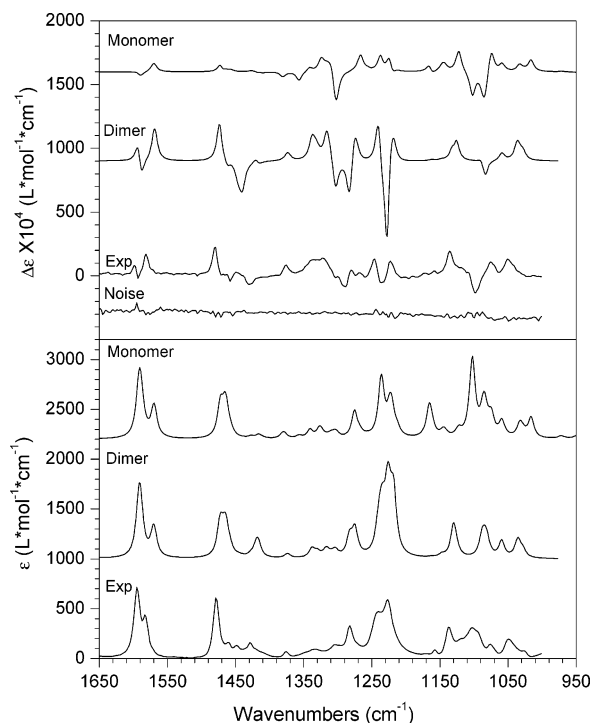


Figure 2. Comparison between experimental and B3LYP/6-31G* predicted vibrational absorption (bottom panel) and VCD (top panel) spectra of 2-(3-chlorophenoxy)propanoic acid. The predicted frequencies are scaled by 0.9613. The experimental measurements were made for (+)-enantiomer and calculations were done for (*R*)-configuration. The trace labeled “noise” represents the reproducibility level in the experimental VCD spectrum.

experimental spectra. (B) (*R*)-2-(3-Chlorophenoxy)propanoic acid, (*R*)-2: The four lowest energy conformers, labeled Con1, Con2, Con3, and Con4, with fractional populations of 0.25, 0.25, 0.23, and 0.20 are identified. The four dihedral angles, D1, D2, D3, and D4, for these conformers are as follows: 177, 71, 36, and 179 for Con1; 0.4, 72, -158, and -177 for Con2; 178, 73, -158, and -177 for Con3; and -2, 70, 33, and 179 for Con4. The population weighted predicted vibrational absorption and VCD spectra are compared to the experimental spectra in Figure 2. From this figure it is evident that the predicted spectra of monomeric (*R*)-2 do not compare well with the experimental spectra for this acid either. (C) (*R*)-2-(4-Chloro-2-methylphenoxy)propanoic acid, (*R*)-3: Two lowest energy conformers, labeled Con1 and Con2 with fractional populations of 0.46 and 0.43, are identified. The four dihedral angles, D1, D2, D3, and D4 for these conformers are as follows: 178, 70, 35, and 179 for Con1 and 180, 72, -156, and -177 for Con2. The population weighted predicted vibrational absorption and VCD spectra are compared to the experimental spectra in Figure 3. From this figure it is evident that the predicted spectra for monomeric (*R*)-3 do not compare well with the experimental spectra. (D) (*R*)-2-(2,4-Dichlorophenoxy)propanoic acid, (*R*)-4: Three lowest energy conformers, labeled Con1, Con2 and Con3 with fractional populations of 0.31, 0.28, and 0.26, are identified. The four dihedral angles, D1, D2, D3, and D4, for these conformers are as follows: 177, 70, 36, and 178 for Con1; 178, 72, -160,

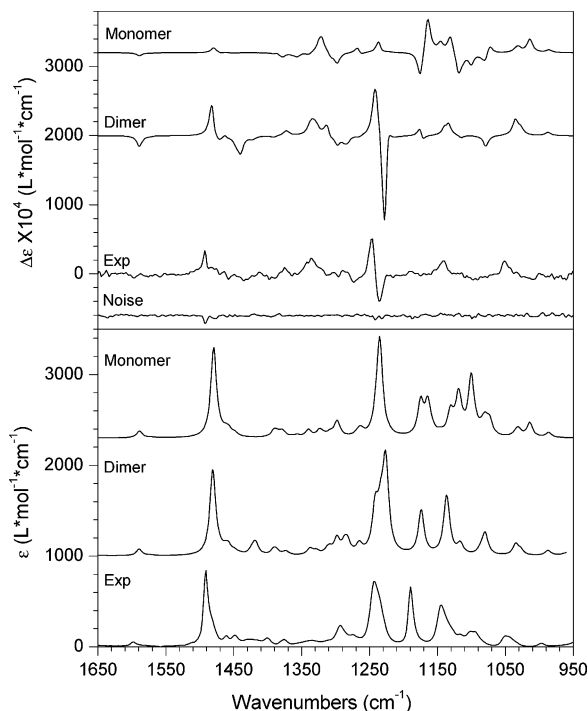


Figure 3. Comparison between experimental and B3LYP/6-31G* predicted vibrational absorption (bottom panel) and VCD (top panel) spectra of 2-(4-chloro-2-methylphenoxy)propanoic acid. The predicted frequencies are scaled by 0.9613. The experimental measurements were made for (+)-enantiomer and calculations were done for (R)-configuration. The trace labeled “noise” represents the reproducibility level in the experimental VCD spectrum.

and -177 for Con2; and 82 , 80 , -171 , and -179 for Con3. The population weighted predicted vibrational absorption and VCD spectra are compared to the experimental spectra in Figure 4. From this figure it is evident that the predicted spectra for monomeric (R)-4 do not compare well with the experimental spectra.

In summary the calculations for monomeric propanoic acids failed to provide a reasonable agreement^{6,7} between the predicted and experimental VA and VCD spectra. However, after methyl esterification of the acids, the experimental VA and VCD spectra obtained for esters were correctly reproduced^{6,7} by the B3LYP/6-31G* predictions of these spectra for the esters. This observation indicated that the mismatch between experimental and predicted spectra for acids is not due to the theoretical level used for the calculations but is likely to be associated with intermolecular hydrogen bonding prevalent for carboxylic acids in solution. The presence of intermolecular hydrogen bonding in solution for the four acids considered is further confirmed^{6,7} by the concentration dependent absorption spectra. Although methyl esterification^{6,7} removed the hydrogen bonding influence in the experimental spectra and provided a good match between experimental and predicted spectra for esters, this approach does not answer the question about the predominant conformations of acids in solution, which is critical to explain the biological activity of acids. Thus we found it necessary to pursue calculations on dimer conformations of acids.

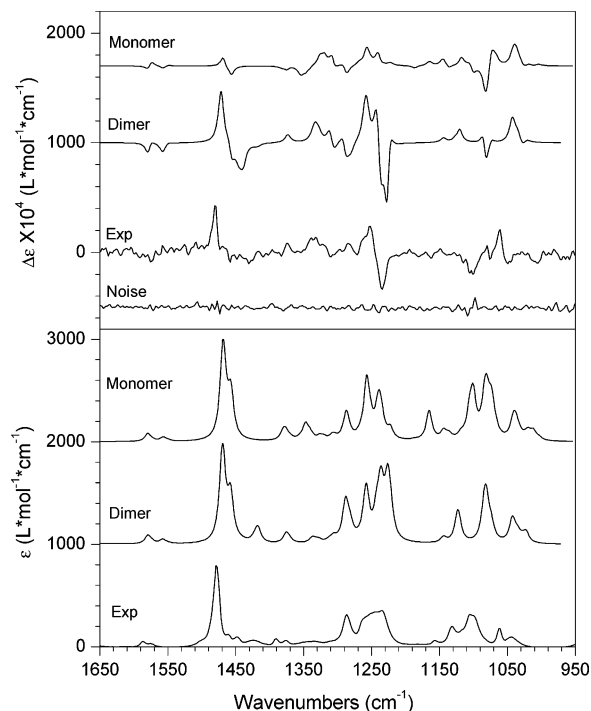
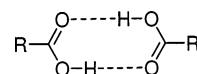


Figure 4. Comparison between experimental and B3LYP/6-31G* predicted vibrational absorption (bottom panel) and VCD (top panel) spectra of 2-(2,4-dichlorophenoxy)propanoic acid. The predicted frequencies are scaled by 0.9613. The experimental measurements were made for (+)-enantiomer and calculations were done for (R)-configuration. The trace labeled “noise” represents the reproducibility level in the experimental VCD spectrum.

Chart 2. Carboxylic Acid Dimer



Dimer Conformations. It is known that carboxylic acids tend to form dimers via intermolecular hydrogen bonding between two monomer units, as shown in Chart 2. The problem in constructing dimer conformations for the four acids under consideration is that these acids have too many possible starting conformations for monomers, making the calculations for dimers a tedious task. To construct a dimer conformation, the dihedral angle, D4, of $C^8C^9O^{10}H^{11}$ (see Chart 1) can be fixed at ~ 180 degree, but there are three other dihedral angles, D1, D2, and D3, which can be varied. If we take 60 , 180 , and -60 as possible starting angles for each of these three dihedral angles, then one has to consider 27 starting structures for each monomer unit in the dimer. Combining the two monomer units, the dimer formed will then have a total of $(27+1)*27/2 = 378$ possible starting conformations for each of the four acids considered.

However, upon looking at the predicted lowest energy conformers of monomeric acids and their methyl esters,^{6,7} we found that the dihedral angles D1, D2, and D3 of lowest energy conformers of monomeric acids and their esters are similar. Based on this observation, we developed the following working hypothesis for constructing dimer conformations. Since the dihedral angles D1, D2, and D3 are not influenced significantly by esterification, they probably

Table 1. Optimized Geometries, Gibbs Energies, and Populations of Conformers of (*R*)-2-(2-Chlorophenoxy)propanoic Acid Dimer^a

conformer	monomer 1				monomer 2				energy (kJ/mol)	population
	D1	D2	D3	D4	D1	D2	D3	D4		
Con3-Con4	178	72	-159	-176	79	81	-169	-177	0	0.3366
Con3-Con3	177	72	-154	-176	177	72	-154	-176	1.696	0.1698
Con1-Con3	176	71	35	178	178	72	-155	-176	1.859	0.1590
Con1-Con4	177	71	31	178	79	81	-169	-178	2.308	0.1326
Con1-Con1	177	72	32	178	177	72	32	178	2.977	0.1013
Con4-Con4	79	80	-167	-177	79	80	-167	-177	2.990	0.1007

^a The labels Con1, Con2, Con3, and Con4 are for the optimized conformations of monomeric acid. The dihedral angle definitions for D1, D2, D3, and D4 are respectively, C²C¹O⁷C⁸, C¹O⁷C⁸C⁹, O⁷C⁸C⁹O¹⁰, and C⁸C⁹O¹⁰H¹¹. See Chart 1 for atom numbering. The four optimized dihedral angles, D1–D4, for monomeric acid conformers are as follows: 177, 71, 35, and 178 for Con1; -164, 146, -4, and 1 for Con2; 177, 73, -159, and -176 for Con3; and 81, 80, -169, and -178 for Con4.

would not be influenced by hydrogen bonding as well. Then the lowest energy conformers of monomeric acids can be used to represent the monomer units in a dimer. This hypothesis, along with the requirement that the C⁸C⁹O¹⁰H¹¹ dihedral angle, D4, should be ~180° for intermolecular hydrogen bonding, will greatly reduce the number of possible starting dimer conformations. With these guidelines, we have investigated the possible dimer conformations using the lowest energy monomeric acid (or their ester) conformations as the starting point. The notation used for dimers is as follows: if a dimer is formed from combining conformer 1 (labeled Con1) of one monomer unit and conformer 3 (Con3) of a second monomer unit, then the dimer is labeled as Con1-Con3. The reliability of final dimer conformations is then evaluated by comparing the predicted VA and VCD spectra for these conformers with the corresponding experimental spectra in solution.

(A) (*R*)-2-(2-Chlorophenoxy)propanoic Acid, (*R*)-**1**. For (*R*)-**1**, we constructed the dimer conformations using the optimized structures of conformers 1, 3, and 4 of the monomeric acid⁷ (labeled as Con1, Con3, and Con4). The structures of these three conformations are similar to those of conformers 1, 2, and 3 of methyl ester.⁷ The conformer 2 of monomeric acid was not used because the dihedral angle D4 for this conformer (1.2°) does not permit dimer formation. The length of hydrogen bond O—H...O is taken from the literature²¹ to be 2.70 Å. The three starting monomer conformations generated six starting dimer conformations, and all of these conformers were submitted to geometry optimization. The final optimized structures are summarized in Table 1. In the optimized structures, the geometries of individual monomer units of dimer are very close to those of starting monomeric acids. The optimized hydrogen bond length, O—H...O, is around 2.69 Å. The optimized structure of lowest energy dimer conformer, Con3-Con4, is shown in Figure 5 A.

To evaluate if these dimer conformers are in fact the ones that represent the spectra in solution, we calculated the vibrational frequencies and intensities for the six stable dimer conformers listed in Table 1. From the vibrational frequency calculation, we noted that all six structures represent energy minima, as there were no imaginary frequencies. The relative Gibbs free energies and populations generated there from are also listed in Table 1. The population weighted VA and VCD spectra for (*R*)-**1** are compared to the corresponding experimental spectra in Figure 1.

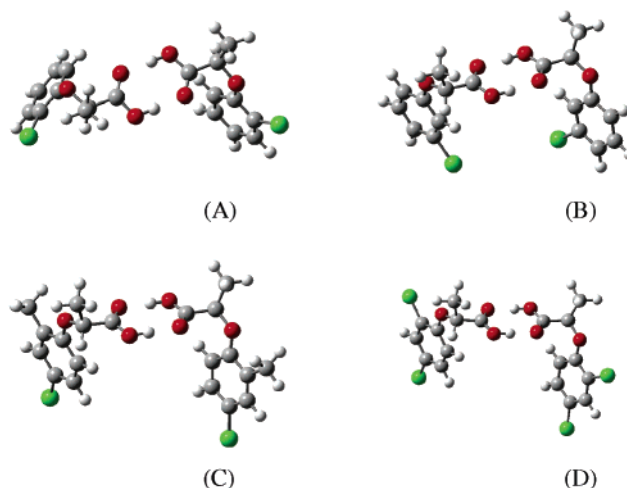


Figure 5. The structures of lowest energy conformers of dimeric acids: (A) Con3-Con4 of (*R*)-2-(2-chlorophenoxy)propanoic acid; (B) Con2-Con2 of (*R*)-2-(3-chlorophenoxy)propanoic acid; (C) Con2-Con2 of (*R*)-2-(4-chloro-2-methylphenoxy)propanoic acid; and (D) Con2-Con2 of (*R*)-2-(2,4-dichlorophenoxy)propanoic acid.

In the VA spectra of Figure 1, the predicted dimer spectra can be seen to be in much better agreement with experimental spectrum, while predicted monomeric acid spectrum is not. The region from ~1650 cm⁻¹ to 1000 cm⁻¹ has a good agreement between experimental and predicted dimer spectra. The predicted monomer VA spectrum on the other hand shows two extra peaks around 1340 and 1160 cm⁻¹. In the VCD spectra of Figure 1, the predicted dimer spectrum has a much better agreement, compared to the spectrum calculated for monomeric acid, with the experimental spectrum in the ~1600–1000 cm⁻¹ region. One discrepancy is in the region near 1275 cm⁻¹ where predicted spectrum shows an extra negative–positive couplet. Nevertheless, the predicted spectrum of dimer satisfactorily reproduces the positive–negative couplet seen around 1240 cm⁻¹ in the experimental spectrum, while the predicted monomer spectrum failed to reproduce this feature. From the calculated vibrational displacements, the vibration that generated this positive–negative couplet is found to involve the hydrogen atoms in the carboxylic groups of dimer. This explains why the predicted spectrum for the monomer acid cannot reproduce this couplet.

Since a reasonable agreement, in both VA and VCD spectra, is seen between the predicted dimer spectra and

Table 2. Optimized Geometries, Gibbs Energies, and Populations of Conformers of (*R*)-2-(3-Chlorophenoxy)propanoic Acid Dimer^a

conformer	monomer 1				monomer 2				energy (kJ/mol)	population
	D1	D2	D3	D4	D1	D2	D3	D4		
Con2-Con2	0.1	73	-158	-176	0.1	72	-158	-176	0	0.1898
Con3-Con3	178	72	-154	-176	179	72	-154	-176	0.181	0.1764
Con2-Con3	0.1	72	-160	-177	179	71	-157	-177	0.328	0.1662
Con3-Con4	178	72	-156	-176	-1	71	32	179	1.000	0.1267
Con1-Con3	177	71	35	178	178	72	-156	-177	1.082	0.1227
Con1-Con2	177	71	33	178	0.1	72	-157	-177	1.166	0.1186
Con2-Con4	-0.4	72	-157	-177	-2	71	33	178	1.599	0.0996

^a The labels Con1, Con2, Con3, and Con4 are for the optimized conformations of monomeric acid. The dihedral angle definitions for D1, D2, D3, and D4 are, respectively, C²C¹O⁷C⁸, C¹O⁷C⁸C⁹, O⁷C⁸C⁹O¹⁰, and C⁸C⁹O¹⁰H¹¹. See Chart 1 for atom numbering. The four optimized dihedral angles, D1–D4, for monomeric acid conformers are as follows: 177, 71, 36, and 179 for Con1; 0.4, 72, -158, and -177 for Con2; 178, 73, -158, and -177 for Con3; and -2, 70, 33, and 179 for Con4.

Table 3. Optimized Geometries, Gibbs Energies, and Populations of Conformers of (*R*)-2-(4-Chloro-2-methylphenoxy)propanoic Acid Dimer^a

conformer	monomer 1				monomer 2				energy (kJ/mol)	population
	D1	D2	D3	D4	D1	D2	D3	D4		
Con2-Con2	180	71	-155	-176	180	71	-155	-176	0	0.5465
Con1-Con2	180	70	33	178	180	71	-156	-176	1.452	0.3042
Con1-Con1	179	71	31	178	179	71	31	178	3.216	0.1493

^a The labels Con1 and Con2 are for the optimized conformations of monomeric acid. The dihedral angle definitions for D1, D2, D3, and D4 are, respectively, C²C¹O⁷C⁸, C¹O⁷C⁸C⁹, O⁷C⁸C⁹O¹⁰, and C⁸C⁹O¹⁰H¹¹. See Chart 1 for atom numbering. The four optimized dihedral angles, D1–D4 for monomeric acid conformers are as follows: 178, 70, 35, and 179 for Con1 and 180, 72, -156, and -177 for Con2.

experimental spectra in solution, the dimer conformations used in calculation can be considered to represent the conformations in the solution. Furthermore, since experimental VCD spectra were obtained for (+)-enantiomer and calculations were done for the (*R*)-configuration, the absolute configuration can be assigned as (+)-(*R*), as was concluded from prior investigations⁷ on methyl ester of this acid.

(*B*) (*R*)-2-(3-Chlorophenoxy)propanoic Acid, (*R*)-**2**. Location of chlorine atom at position 3 of phenyl group in (*R*)-**2** makes the energy barrier less when the dihedral angle C²C¹O⁷C⁸ is varied. As a result there is one additional conformation here than in the case of (*R*)-**1**. Four stable conformers 1, 2, 3, and 4 of monomeric acid are similar⁷ to conformers 1, 2, 4, and 3 of the corresponding methyl ester. These conformers (labeled as Con1, Con2, Con3, and Con4) are used to construct dimer conformers, which lead to 10 starting dimer structures. All of these 10 conformers are submitted to geometry optimization. The seven most stable conformers are listed in Table 2. The remaining three conformers with higher energy are not listed because their populations are negligible for the present purposes. Again, the monomer components in dimer have the geometries similar to those optimized for monomeric acids. The structure of the lowest energy dimer conformer, Con2-Con2, is shown in Figure 5B. The vibrational spectra of (*R*)-**2** dimers are calculated at the optimized geometries. The populations of dimer conformers deduced from Gibbs energies are also listed in Table 2. The VA and VCD spectra are compared to the experimental spectra in Figure 2. In the VA spectra of Figure 2, we see an excellent agreement again between experimental and predicted dimer spectra but not between experimental and predicted monomer spectra. The relative intensities of predicted dimer VCD bands in the 1360 cm⁻¹ to 1200 cm⁻¹ region are somewhat larger than the experimental values. When positive and negative VCD bands appear next to each other, separation between their band

positions will influence their relative intensities due to mutual cancellation. Thus unless band positions are predicted accurately, which is difficult at B3LYP/6-31G* level, the relative intensities of overlapping VCD bands cannot be reproduced well. The overall agreement between experimental and predicted dimer VCD spectra is much better than that between the experimental and predicted monomer VCD spectra. In particular, the signs of VCD bands in predicted dimer and experimental spectra agree very well in the region from ~1650 cm⁻¹ to 1000 cm⁻¹. Thus the dimer conformations used can be considered to represent the conformations in solution. From the comparison between predicted dimer and experimental spectra, the absolute configuration of **2** can be assigned as (+)-(*R*), as concluded from investigations on corresponding methyl esters.⁷

(*C*) (*R*)-2-(4-Chloro-2-methylphenoxy)propanoic Acid, (*R*)-**3**. For this acid, the conformers 1 and 2 (labeled as Con1 and Con2) in both acid and its methyl ester⁶ account for about 90% of the population. Therefore, only conformers 1 and 2 are chosen to construct dimer structures. This will generate three starting dimer structures. All of these three conformers are submitted for geometry optimization. Their optimized structures are listed in Table 3. Here also the monomer components in dimer have the geometries similar to those optimized for monomeric acids. The structure of the lowest energy dimer conformer, Con2-Con2, is shown in Figure 5C.

The VA and VCD spectra are calculated for these three conformers at their optimized geometries. The population weighted predicted spectra for dimeric acids are shown in Figure 3. In the VA spectra of Figure 3, we notice an excellent agreement again between experimental and predicted dimerspectra. There are some minor differences in the relative absorption intensities among predicted dimer and experimental spectra, but the relative intensities cannot be expected to match well at B3LYP/6-31G* level used here. In the VCD spectra of Figure 3, the major positive and

Table 4. Optimized Geometries, Gibbs Energies, and Populations of Conformers of (*R*)-2-(2,4-Dichlorophenoxy)propanoic Acid Dimer^a

conformer	monomer 1				monomer 2				energy (kJ/mol)	population
	D1	D2	D3	D4	D1	D2	D3	D4		
Con2-Con2	178	72	-155	-176	178	72	-155	-176	0	0.2340
Con1-Con2	177	71	31	178	178	72	-158	-176	0.415	0.1979
Con2-Con3	178	73	-162	-176	79	81	-171	-178	0.848	0.1662
Con3-Con3	80	81	-171	-178	80	81	-171	-178	0.898	0.1628
Con1-Con3	177	71	34	178	80	80	-168	-178	1.286	0.1392
Con1-Con1	177	71	32	178	177	71	32	178	2.108	0.0999

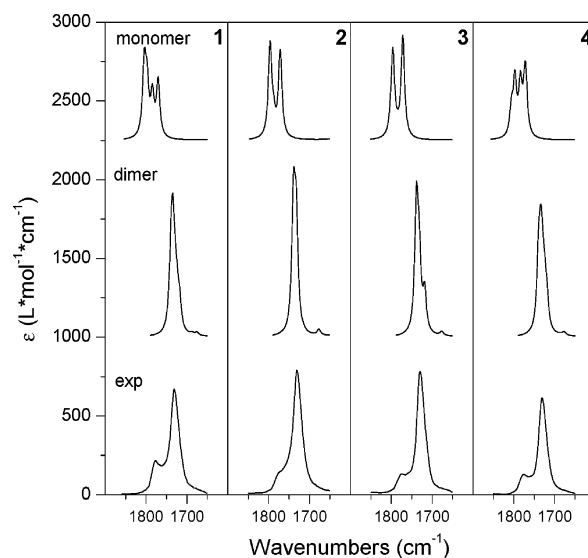
^a The labels Con1, Con2, and Con3 are for the optimized conformations of monomeric acid. The dihedral angle definitions for D1, D2, D3, and D4 are, respectively, C²C¹O⁷C⁸, C¹O⁷C⁸C⁹, O⁷C⁸C⁹O¹⁰, and C⁸C⁹O¹⁰H¹¹. See Chart 1 for atom numbering. The four optimized dihedral angles, D1–D4, for monomeric acid conformers are as follows: 177, 70, 36, and 178 for Con1; 178, 72, -160, and -177 for Con2; and 82, 80, -171, and -179 for Con3.

negative VCD bands agree well between experimental and predicted dimer spectra. The experimental positive–negative VCD couplet around 1240 cm⁻¹, which does not show up in the predicted spectrum of monomeric acid is reproduced very nicely in predicted dimer spectrum. Thus the dimer conformations used can be considered to represent the conformations in solution. Since the signs of VCD bands in predicted dimer and experimental spectra agree very well in Figure 3, the absolute configuration of **3** can be assigned as (+)-(*R*), as deduced from investigations on corresponding methyl ester.⁶

(*D*) (*R*)-2-(2,4-Dichlorophenoxy)propanoic Acid, (*R*)-**4**. For (*R*)-**4**, three conformers (labeled Con1, Con2, Con3) account for most of the population of monomer acid conformers. Thus these three conformers are used to construct the dimer structures, resulting in six starting dimer conformations. The optimized dimer structures are listed in Table 4. Here also the monomer components in dimer have the geometries similar to those optimized for monomeric acids. The structure of the most stable conformer, Con2-Con2, is shown in Figure 5D.

The predicted VA and VCD spectra for dimeric acid are shown in Figure 4. The agreement between experimental and predicted dimer spectra is quite good, while that between experimental and predicted monomer spectra is rather poor. Some minor discrepancies however should be noted. In the 1250 cm⁻¹ region, the experimental absorption spectrum shows a broad band, while the predicted dimer absorption spectrum shows three resolved bands. In the region from 1060 to 1150 cm⁻¹, the predicted dimer spectrum shows two well-separated peaks, while experimental spectrum shows two partially separated peaks. These discrepancies are attributed to the errors in predicted band positions at the B3LYP/631G* level. Nevertheless, the fact the experimental spectra are reasonably well reproduced by the predicted dimer spectra and not by the predicted monomer spectra suggests that the dimer conformations used here represent those in solution. Moreover, since the signs of all major VCD bands in predicted dimer and experimental spectra agree very well, the absolute configuration of **4** can be assigned as (+)-(*R*), agreeing with the conclusion arrived at from the investigations on corresponding methyl ester.⁶

The vibrational absorption spectra in the carbonyl region are shown in Figure 6 for all four acids considered. Concentrations used for the experimental absorption spectra in Figure 6 are the same as those for the spectra in Figures

**Figure 6.** The experimental (bottom trace) and predicted (top two traces) vibrational absorption spectra for acids **1–4** in the carbonyl region. The predicted frequencies are scaled by 0.9613.

1–4. The experimental VCD spectra in this region are not shown because VCD bands in this region are very weak. The predicted dimer absorption spectra have better agreement with experimental absorption spectra compared to the predicted monomer spectra. The strong peak around 1730 cm⁻¹ in the experimental spectra is reproduced well in the predicted dimer spectra. The high frequency shoulder at 1774 cm⁻¹ in the experimental spectra is assigned⁷ to the carbonyl vibration of monomer. Although some amount of monomer conformers is present in solution, the absorption and VCD in the 1650–950 cm⁻¹ region are mostly determined by the dimer conformations as can be inferred from Figures 1–4 and from concentration dependent studies (vide infra). If the goals were to compare the experimental and calculated spectra quantitatively, then one would have to simulate the predicted spectra with a certain amount of monomer conformers. Alternately, it would be possible to determine the percent populations of monomers and dimers using a regression analysis of the experimental and predicted intensities,²² if the predicted absorption and VCD intensities are quantitatively accurate. But it was pointed out²² that B3LYP predictions of absorption and VCD intensities are not sufficiently accurate for quantitative comparisons, even when large basis sets are used for small molecules. For this reason

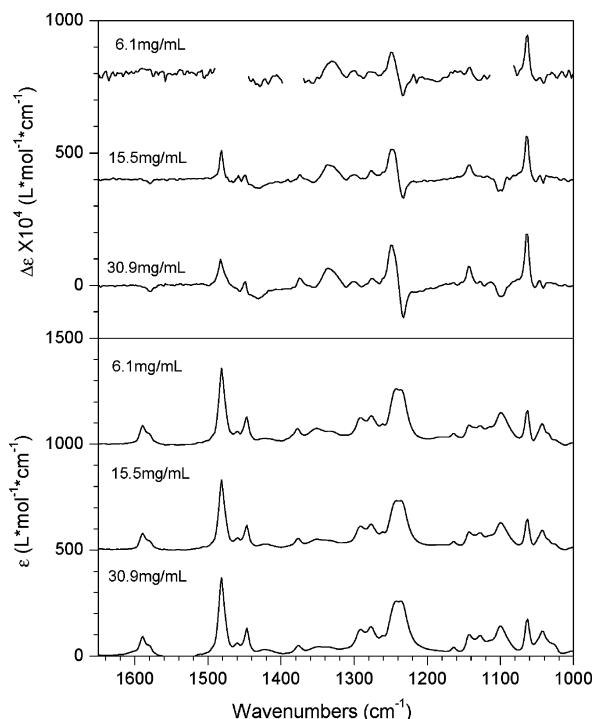


Figure 7. Concentration dependent vibrational absorbance and VCD spectra of (+)-2-(2-chlorophenoxy)propanoic acid in CDCl_3 . The path length is $180\ \mu\text{m}$ for $30.9\ \text{mg/mL}$, $400\ \mu\text{m}$ for $15.5\ \text{mg/mL}$, and $900\ \mu\text{m}$ for $6.1\ \text{mg/mL}$. In the topmost VCD spectrum (at $6.1\ \text{mg/mL}$) the regions around 1470 , 1360 , and $1080\ \text{cm}^{-1}$ have been removed because of noise resulting from solvent absorption interference.

we did not attempt to obtain the simulated spectra with an admixture of monomer and dimer contributions.

Concentration Dependence. It is known that studies on dilute solutions are appropriate to avoid the influence of dimers and to increase the population of monomers in solution. This strategy, although perfectly valid, is not particularly useful for VCD spectra because, extremely dilute concentrations are needed for realizing predominant monomer conformations and at such dilute concentrations solvent absorption interference prevents VCD measurements with sufficient signal-to-noise. To illustrate this point concentration dependent absorption and VCD spectra for (+)-2-(2-chlorophenoxy)propanoic acid in the 1650 – $950\ \text{cm}^{-1}$ region are shown in Figure 7. As the concentration is lowered, the VCD signal magnitudes are seen to decrease, but the onset of solvent interference becomes an issue long before monomer contributions begin to appear in the region studied. As can be seen in Figure 7, the regions 1491 – 1445 , 1398 – 1369 , and 1115 – $1082\ \text{cm}^{-1}$ had to be blocked out at a concentration of $6.1\ \text{mg/mL}$, due to excessive noise resulting in these regions from the solvent absorption interference. Thus it is not possible to conduct VCD studies on solutions that are continuously diluted to the point where monomers dominate.

Spectral Additivity. When dealing with large molecular systems, it would be tempting to undertake the calculations on different fragments of the molecule of interest and add the results to represent the property of full molecule. Such an approach would be valid if the interactions between

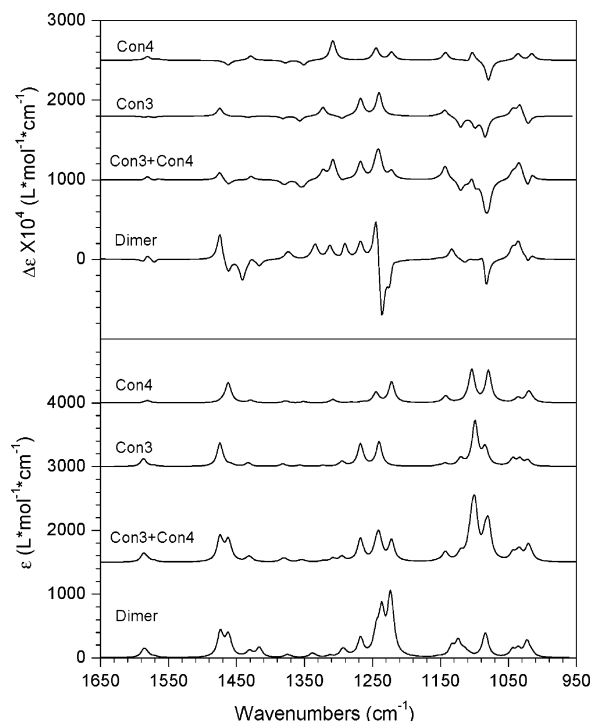


Figure 8. Evaluation of spectra additivity of B3LYP/6-31G* predicted spectra for 2-(2-chlorophenoxy)propanoic acid: (a) vibrational absorption (bottom panel) and (b) VCD (top panel) Con3 and Con4 are the monomer spectra predicted for these two conformations. Con3+Con4 represents the numerical sum of the spectra predicted for monomer conformers 3 and 4, while dimer spectra represent those predicted for the dimer Con3-Con4. The predicted frequencies are scaled by 0.9613 .

different fragments do not influence the property of interest. In the case of vibrational properties, however, the very nature of normal coordinates imposes cross talk between fragments of a molecule. So it is of interest to know if the vibrational spectra of fragments can be additive to represent the vibrational spectrum of full molecules. Since dimers are viewed as a combination of two monomers, it would be useful to verify the additivity of the spectra of monomers. In Figure 8, the predicted vibrational spectra for monomer conformers 3 and 4, their numerical sum and of dimer derived from these monomers are compared for 2-(2-chlorophenoxy)propanoic acid. In the 1150 – $950\ \text{cm}^{-1}$ region, the numerically added VCD spectrum compares reasonably well with the predicted VCD spectrum of dimer. But the numerically added absorption spectrum in this region does not match with the predicted absorption spectrum of dimer. In the 1400 – $1150\ \text{cm}^{-1}$ region, both absorption and VCD spectra predicted for dimer are significantly different from the corresponding numerically added spectra for monomers contained therein. The vibrational modes involving intermolecular hydrogen bonding appear in the 1400 – $1150\ \text{cm}^{-1}$ region, as noted for other hydrogen-bonded systems²³ such as butanol. Thus the concept of additivity for vibrational absorption and VCD spectra of α -aryl propanoic acids does not work in the spectral regions where vibrational modes involving intermolecular hydrogen bonds occur.

Conclusions

The predicted VA and VCD spectra for monomer conformations of α -aryloxypropanoic acids did not reproduce the corresponding experimental spectra. This is believed to be due to dimer formation for acids in solution. Noting that the predicted structures of monomeric acids are very similar to those of corresponding methyl esters, we hypothesized that the lowest energy structures of monomeric acids can be used to construct the starting structures for dimeric acids. The starting geometries of dimer structures were optimized at B3LYP/6-31G* level. In the optimized dimer structures, the individual monomer components are found to have structures similar to the optimized conformers of monomeric acids. To verify the reliability of optimized dimer structures, VA and VCD spectra have been calculated at the optimized geometries. The population weighted predicted VA and VCD spectra for dimeric acids are found to be in good agreement with the corresponding spectra in CDCl_3 solution.

Based on the present work, we can suggest a general approach for interpreting the vibrational spectra of carboxylic acids in solution. This approach involves first finding the lowest energy conformers of a monomeric acid and its methyl ester. If the lowest energy conformers of acid and its ester are similar, then one can use these lowest energy optimized structures for generating dimer conformers. Vibrational spectra calculated for the optimized dimer conformers can then be compared to the experimental spectra to evaluate the validity of these conformers in solution. In this manner, one can determine the predominant conformations of dimeric acids as well as their absolute configuration using density functional predictions of VA and VCD spectra.

Acknowledgment. Grants from NSF (CHE0092922) and Vanderbilt University are gratefully acknowledged. We thank Jeremy Wardman of A.H. Marks Co., for providing the analytical grade samples of Mecoprop and Dichloropop. Contract grant sponsor: NSF; contract grant number: CHE0092922.

Supporting Information Available: Optimized coordinates, vibrational frequencies, and intensities for lowest energy conformers are provided. This material is available free of charge via the Internet at <http://pubs.acs.org>.

References

- (1) Buser, H. R.; Muller, M. D. *Environ. Sci. Technol.* **1997**, *31*, 1960–1967.
- (2) Sheldon, R. A. *Chirotechnology: Industrial Synthesis of Optically Active Compounds*; Marcel Dekker: New York, 1993; pp 62–64.
- (3) Loos, M. A. *Herbicides: Chemistry, Degradation and Mode of Action*; Marcel Dekker: New York, 1975; Vol. 1, pp 1–128.
- (4) Testa, B.; Trager, W. F. *Chirality* **1990**, *2*, 129–133.
- (5) Zipper, C.; Suter, M. J. F.; Haderlein, S. B.; Gruhl, M.; Kohler, H. P. E. *Environ. Sci. Technol.* **1998**, *32*, 2070–2076.
- (6) He, J.; Wang, F.; Polavarapu, P. L. *Chirality* **2005**, *17*, S1–S8.
- (7) He, J.; Polavarapu, P. L. *Spectrochim Acta* **2005**, in press.
- (8) Jeffrey, G. A. *An introduction to hydrogen bond*; Oxford University Press: New York, 1997.
- (9) Watson, J. D.; Crick, F. H. C. *Nature* **1953**, *171*, 737–738.
- (10) Pauling, L.; Corey, R. B.; Branson, H. R. *Proc. Natl. Acad. Sci. U.S.A.* **1951**, *37*, 205–211.
- (11) Scheiner, S. *Hydrogen bond, a theoretical perspective*; Oxford University Press: New York, 1997; pp 99–101.
- (12) Hadzi, D. *Theoretical treatments of hydrogen bonding*; John Wiley & Sons: 1997; pp 13–74.
- (13) Barron, L. D. *Molecular Light Scattering and Optical Activity*, 2nd ed.; Cambridge University Press: 2004; pp 331–342.
- (14) Polavarapu, P. L. *Vibrational spectra: principles and applications with emphasis on optical activity*; Elsevier: New York, 1998; pp 143–182.
- (15) Nafie, L. A. *Annu. Rev. Phys. Chem.* **1997**, *48*, 357–386.
- (16) (a) Polavarapu, P. L.; He, J. *Anal. Chem.* **2004**, *76*, 61A–67A. (b) Freedman, T. B.; Cao, X.; Dukor, R. K.; Nafie, L. A. *Chirality* **2003**, *15*, 743–758. (c) Devlin, F. J.; Stephens, P. J.; Osterle, C.; Wiberg, K. B.; Cheeseman, J. R.; Frisch, M. J. *J. Org. Chem.* **2002**, *67*, 8090–8096. (d) Andrushchenko, V.; van de Sande, J. H.; Wieser, H. *Biopolymers* **2003**, *72*, 374–390. (e) Keiderling, T. A.; Xu, Q. *Adv. Protein Chem.* **2002**, *62*, 111–161.
- (17) (a) Wang, F.; Polavarapu, P. L.; Drabowicz, J.; Kielbasinski, P.; Potrzebowski, M. J.; Mikolajczyk, M.; Wieczorek, M. W.; Majzner, W. W.; Lazewska, I. *J. Phys. Chem.* **2004**, *108*, 2072–2079. (b) Cappelli, C.; Corni, S.; Mennucci, B.; Cammi, R.; Tomasi, J. *J. Phys. Chem. A* **2002**, *106*, 12331–12339.
- (18) Nafie, L. A. *Appl. Spectrosc.* **2000**, *54*, 1634–1645.
- (19) M. J. Frisch, G. W. T., H. B. Schlegel, G. E. Scuseria, M. A. Robb, J. R. C., J. A. Montgomery, Jr., T. Vreven, K. N. Kudin, J. C. B., J. M. Millam, S. S. Iyengar, J. Tomasi, V. Barone, B. M., M. Cossi, G. Scalmani, N. Rega, G. A. Petersson, H. N., M. Hada, M. Ehara, K. Toyota, R. Fukuda, J. H., M. Ishida, T. Nakajima, Y. Honda, O. Kitao, H. Nakai, M. K., X. Li, J. E. Knox, H. P. Hratchian, J. B. Cross, C. Adamo, J. J., R. Gomperts, R. E. Stratmann, O. Yazyev, A. J. Austin, R. C., C. Pomelli, J. W. Ochterski, P. Y. Ayala, K. Morokuma, G. A. V., P. Salvador, J. J. Dannenberg, V. G. Zakrzewski, S. D., A. D. Daniels, M. C. Strain, O. Farkas, D. K. M., A. D. Rabuck, K. Raghavachari, J. B. Foresman, J. V. O., Q. Cui, A. G. Baboul, S. Clifford, J. Cioslowski, B. B. S., G. Liu, A. Liashenko, P. Piskorz, I. Komaromi, R. L. M., D. J. Fox, T. Keith, M. A. Al-Laham, C. Y. Peng, A. N., M. Challacombe, P. M. W. Gill, B. Johnson, W. C., M. W. Wong, C. Gonzalez, and J. A. Pople. Gaussian 03, Revision B.01; Gaussian, Inc.: Pittsburgh, PA, 2003.
- (20) Wong, M. W. *Chem. Phys. Lett.* **1996**, *256*, 391–399.
- (21) Almenningen, A.; Bastiansen, O.; Motzfeldt, T. *Acta Chem. Scand.* **1969**, *23*, 2848–2864.
- (22) He, J.; Petrovic, A. G.; Polavarapu, P. L. *J. Phys. Chem.* **2004**, *108*, 1671–1680. He, J.; Petrovic, A. G.; Polavarapu, P. L. *J. Phys. Chem B* **2004**, *108*, 20451–20457.
- (23) Wang, F.; Polavarapu, P. L. *J. Phys. Chem. A* **2000**, *104*, 10683–10687.